CHAPTER 5

LIQUID-SOLID CONTACTING IN A PILOT REACTOR

The literature review in Chapter 2 illustrates the importance of wetting efficiency measurements under reaction conditions relevant to typical industrial applications. All the reactor measurements of wetting efficiency are accompanied by some estimation of the kinetic expression of the catalysed reaction, and most are also dependent on a correlation-based estimation of external mass transfer. In this chapter, measurements of wetting efficiency and liquid-solid mass transfer coefficients are derived from reactor conversion data. Data include measurements for gas-liquid upflow, and different hydrodynamic states in trickle flow. Based on the theoretical insights from Chapter 4 regarding the behaviour of eggshell catalysts, typical conditions are identified for a reaction system where wetting efficiency and liquid-solid mass transfer effects can easily be recognised. These theoretical considerations are also useful for the identification of other possible reaction systems suitable for the proposed wetting efficiency measurement methods. A reaction study at such conditions in a high-pressure, 50 mm I.D. pilot reactor is then performed to obtain wetting efficiency and liquid-solid mass transfer coefficient measurements. As in Chapter 3, both boundaries of hydrodynamic multiplicity in pre-wetted beds are explored.

Approximations of the reported parameters are based on conversion data for two reactions: hydrogenation of linear octenes and hydrogenation of isooctenes (trimethylpentenes, or TMP). These reactions find their application in the Fischer-Tropsch refining industry (de Klerk, 2008): Fischer-Tropsch naphtha contains up to 85% olefins, and requires severe hydrogenation. This leads to a drastic decrease in the motor octane number (MON) of the treated process stream. The decrease in MON is highly dependent on the molecular structure of the hydrogenated olefin. As a rule, the hydrogenation of linear olefins leads to a more severe drop in the octane number than the hydrogenation of branched olefins. It

is therefore preferable to hydrogenate the branched olefins and retain the least-branched olefinic molecules.

5.1 Finding an applicable reaction system

5.1.1 Theoretical considerations

For a simple estimation of liquid-solid contacting effects, it is first necessary to identify conditions where reactor performance is linked in a simple way with wetting efficiency. From the previous chapter, the overall particle efficiency for a first-order liquid-limited reaction is given by the form[1]:

$$\eta_0 = \eta\left(1 + \frac{\phi_G^2}{Bi'.f}\eta\right)^{-1}$$
$$\text{where: } Bi' = \frac{V_R k_{LS}}{S_p D_{eff}} \quad \phi_G = \frac{V_R}{S_p}\sqrt{\frac{k_r}{D}_{eff}} \tag{5.1}$$

A linear dependence of η_0 on f is ideal for the measurement of average wetting efficiency, since the PWD in the reactor will then not influence η_0. Theoretically, there are three possible cases where the overall reactor performance is linearly dependent on f over the whole f-range:

1. $\frac{\phi_G^2}{Bi'}\eta \gg 1$ so that $\eta_0 = f\frac{Bi'}{\phi_G^2}$. In this case, the reaction rate is completely external mass transfer limited.

2. $\eta = k \cdot f$ so that $\eta_0 = k \cdot f\left(1 + \frac{\phi_G^2 k}{Bi'}\right)^{-1}$. Here, the reaction is internal diffusion limited, while external mass transfer limitations can also play a role. For an internal mass transfer limited system, $k \approx 1/\phi_G$.

A typical mass transfer study would employ case (1), using a very rapid reaction to measure mass transfer rates. It is, however, not possible to measure wetting efficiency and mass transfer independently when only case (1) is applicable to the system, even if it is possible to vary ϕ_G without changing the hydrodynamics of the reactor. For case (2), or a combination of case (1) and case (2), it is possible to distinguish between the effects of wetting efficiency and liquid-solid mass transfer by varying ϕ_G without changing hydrodynamic conditions in the reactor. Morita and Smith (1978) did this by repeating trickle-bed experiments (i.t.o hydrodynamic conditions) with catalysts of different activities. This requires reactor repacking, stable well-characterised catalysts and good hydrodynamic repeatability. An easier method is to perform two reactions of

[1]The previous chapter frequently deals with different particle shapes, and different forms of this equation are given. The equation shown here is valid for all shapes due to the definitions of Bi' and ϕ_G.

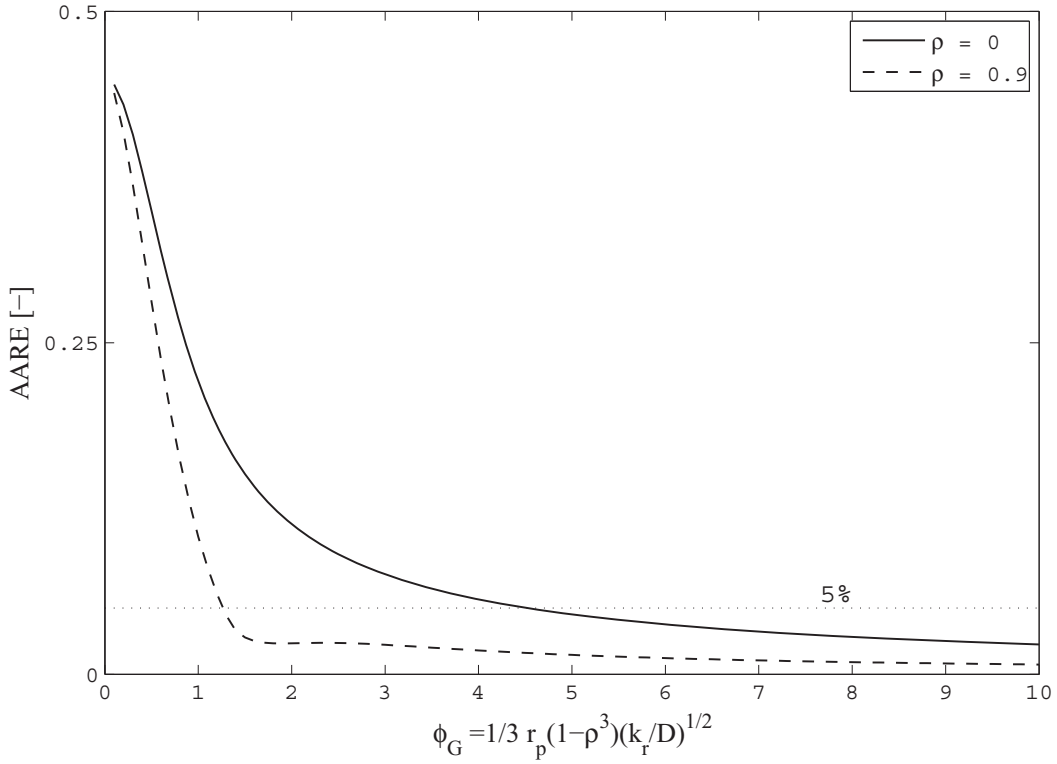

Figure 5.1: Absolute average relative errors obtained when approximating the relationship between η and f for a given ϕ_G as being linear over the whole f-range, as a function of ϕ_G. Errors are calculated by comparing the modified GC model to the linear model $\eta = f \times \eta|_{f=1}$ and are reported for monodispersed and eggshell spherical particles.

different rates in parallel during the same experimental run, giving rise to measurements for two different moduli, $\phi_{G1} > \phi_{G2}$. This approach is followed in the experimental work presented in this chapter. Since k_{LS} and therefore Bi' is not dependent only on the hydrodynamic behaviour of the system, but also of molecular diffusivity of the reagents, care should be taken that both reagents have more or less the same diffusivity, so that $Bi'_1 = Bi'_2 = Bi'$. If this is not the case, it will still not be possible to decouple Bi'_1, Bi'_2 and f. This is dealt with in the next section. The faster reaction corresponding to ϕ_{G1} will be more affected by liquid solid mass transfer (in the limit corresponding to case 1) than the slower reaction (ϕ_{G2}), where the effect of wetting efficiency on particle efficiency will be more prominent. This slower reaction therefore has to comply with case (2), and the particle efficiency should be linearly dependent on f. This is the first requirement on the system. Making use of the modified GC model developed in the Chapter 4 from FEM simulation, one can get an idea for which values of ϕ_G the particle efficiency will be linearly related to f. As shown in Figure 5.1, these values are $\phi_G > 1.5$ for eggshell particles with $\rho = 0.9$ (which are used in this study) and $\phi_G > 4.5$ for monodispersed spherical catalysts.

Where the first requirement stated in the beginning of this chapter is met as long as $\phi_{G2} > 1.5$, the second requirement, i.e. easy decoupling of Bi' and f, requires the slow reaction (ϕ_{G2}) to be slow enough to ensure that it is not completely limited by the resistance to external mass transfer. Say, for internal mass transfer effects to be discernible, overall rate of the slowest reaction should be at least 20% less than it would have been, had it been completely mass tranfser limited. Then:

$$\eta_0 \leq 0.8 f \frac{Bi'}{\phi_{G2}^2}$$

$$\eta \left(1 + \frac{\phi_{G2}^2}{Bi' f}\eta\right)^{-1} \leq 0.8 f \frac{Bi'}{\phi_{G2}^2}$$

$$\text{And:} \quad \eta \approx \frac{f}{\phi_{G2}}$$

$$\therefore \frac{f}{\phi_{G2}} \left(1 + \frac{\phi_{G2}}{Bi'}\right)^{-1} \leq 0.8 f \frac{Bi'}{\phi_{G2}^2}$$

$$\left(1 + \frac{\phi_{G2}}{Bi'}\right)^{-1} \leq 0.8 \frac{Bi'}{\phi_{G2}}$$

$$\therefore \phi_{G2} \leq 4Bi' \tag{5.2}$$

Where according to most correlations, this criterion is easily met for monodispersed particles (Bi is typically larger than 10, see Chapters 2 and 4), it is much more stringent for eggshell particles. Remember that Bi' is per definition proportional to the ratio of reaction volume to external surface area (see Equation 5.1). This is much less for an eggshell catalyst than for a monodispersed one. For example, if it can be safely assumed that for a monodispersed sphere $Bi = k_{LS} \times r_p / D_{eff} \geq 10$, then for an eggshell catalyst $Bi' \geq 10/3 \times (1 - \rho^3)$. Hence for the eggshell catalyst used in this investigation, it is required from equation (5.2) that $\phi_{G2} \leq 3.6$.

A summary of the approximate conditions to meet the first two requirements in the beginning of this chapter is given in Table 5.1, for monodispersed and eggshell catalysts ($\rho = 0.9$). It is clear that monodispersed particles are more suitable for the identification of wetting efficiency than eggshell catalysts. The other three requirements listed in the beginning of this chapter, and other hydrodynamic considerations such as dispersion and possible rate limitations imposed by the gaseous reagent, are dealt with in section 5.3.

Table 5.1: Approximate requirements for the reaction system.

Monodispersed catalyst	Eggshell catalyst used in this study ($\rho = 0.9$)
Diffusivities of both liquid reagents in the solvent should be the same	Same as for monodispersed
First-order reactions	First-order reactions
$4.5 \leq \phi_{G2} \leq 13$	$1.5 \leq \phi_{G2} \leq 3.6$
$\phi_{G1} \gg \phi_{G2}$	$\phi_{G1} \gg \phi_{G2}$

5.2 Reaction system characteristics

The trickle-bed reaction most often encountered in industry is hydrogenation, predominantly for hydrotreatment in the refining of crude oil (Gianetto and Specchia, 1992). Hydrotreatment is characterised by high conversions and low reagent concentrations. An exception to this rule is encountered in high temperature Fischer-Tropsch refineries: HTFT naphtha contains up to 85% olefins, which need to be decreased to $< 18\%$ (de Klerk, 2008). This corresponds to a rather low conversion of approximately 0.8 and since not all of the olefins need to be hydrogenated, it was suggested that some way should be found to selectively hydrogenate the branched olefins rather than linear olefins in the feed stream, to maximise the octane number of the refined naphtha. This study focuses on reactor hydrodynamics and therefore does not further elaborate on this rather interesting problem (due to molecular structure, linear olefins are by nature more rapidly hydrogenated than branched olefins). Nevertheless, a similar reaction system has been selected for the trickle-bed study, mainly because of the large difference in the hydrogenation rates of branched and linear olefins and the fast rate of the hydrogenation of linear olefins in the naphtha boiling range.

The model reactions of this process have been chosen as (i) the hydrogenation of linear octenes, and (ii) the hydrogenation of isooctenes. According to the Wilke-Chang equation, this reaction system meets the requirement of equal diffusivities for both reagents, since the molar masses and densities are equal. Mixtures of all isomers of these reagents are used, so that these are in fact more than two reactions that yield only two paraffinic products. It should therefore be ensured that all reactions leading to the same product can be modelled as one reaction. Also, both reactions should be first-order, for easy modelling of the effect of wetting efficiency on internal diffusion.

The reaction mixture contains roughly 1% linear octene isomers and 2% isooctene isomers in a C_{14}-C_{20} paraffin solvent. Concentrations had to be this low for the trickle-bed reactor to run isothermally while useful conversions can be measured. Physical properties of the reaction mixture are listed in Table 5.2.

Table 5.2: Liquid reaction mixture properties.

Property	Estimated value	Estimation method
Viscosity	1.71 mPa.s	van Velzen et al. (1972) Kendall (1917)
Surface tension	27 $^{mN}/_{m}$	Sugden (1924)
Density	765 $^{kg}/_{m^3}$	Measured
Reagent molecular diffusivity in solvent		Wilke and Chang (1955)
Linear octenes	1.13×10^{-9} $^{m^2}/_{s}$	
Isooctenes	1.13×10^{-9} $^{m^2}/_{s}$	
Average molar mass	$\sim$230 $^{kg}/_{kmol}$	Estimated from GC analysis

A 0.3% Pd/Al_2O_3 spherical eggshell catalyst with a diameter of 3 mm was used to catalyse the reactions. The catalyst was supplied by Heraeus, and is marketed as a hydrogenation catalyst. Particle density is $\pm$ 1100 $^{kg}/_{m^3}$. Shell thickness was determined with a microscope at 0.3 mm.

To characterise the kinetic sytem, batch experiments were performed in a 450 ml Parr autoclave reactor with the temperature controlled ($\pm$ 1 °C) at 60 °C, measuring conversion versus time. The catalyst was crushed to approach intrinsic kinetics. Liquid reagent starting concentrations were the same as in the packed-bed experiments. Before sampling, the sampling line was purged twice with the liquid in the reactor. After completion of the experiment, the total volume of sampled or purged liquid was less than 5% of the total reactor volume. Concentration versus time profiles obtained from sampling of the liquid at different time intervals are shown in figure 5.2. At a given pressure, both reactions are first-order with respect to the liquid reagent. It is clear from the figure that reaction rates are affected by H_2 partial pressure. Packed-bed conversion data will therefore be treated using a first-order rate expression, with a pseudo rate constant that is a function of the H_2 partial pressure. This approach is only valid if the liquid in the packed bed is saturated with H_2 throughout the bed. Care should therefore be taken with separate reactor experiments that this is indeed the case.

At 60 bar and 60°C, the reactions comply with the requirements listed in section 5.1.1. At this pressure and temperature, the first-order rate constant for isooctene hydrogenation is $k_{r2} \approx 0.3\ s^{-1}$, based on the catalyst shell volume. This corresponds to a particle modulus[2] of $\phi_{G2} \approx 2.6$. The rate of hydrogenation of the linear octenes is not very important, as long as it is much faster than that of the isooctenes, which is clearly the case ($k_{r1} \approx 6s^{-1}$, $\phi_{G1} \approx 12$).

The figure also confirms that all linear octene isomers can be viewed as one reagent: since almost pure 1-octene was used as reagent, the linear octene isomer composition changed during the experiment, which clearly did not affect the rate of octane production.

[2]To approximate the generalised modulus, an approximation of the effective diffusivity is necessary. The approximation is based on a particle porosity of 0.8, a tortuosity of $\sqrt{2}$, and a constriction factor of 0.8. See Levenspiel (2006).

The same applies to the isooctene reaction mixture.

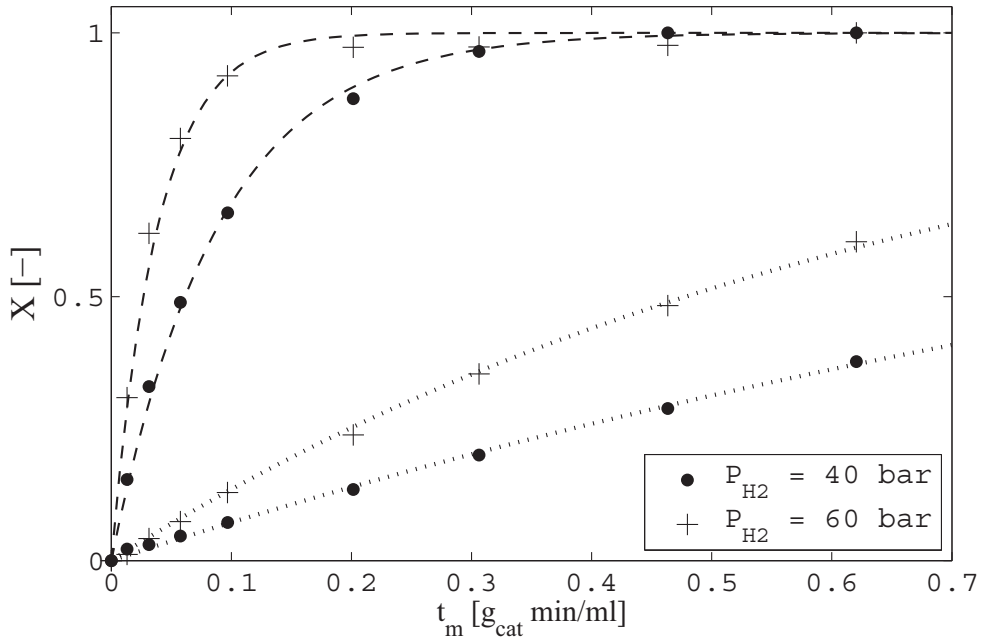

Figure 5.2: Reaction kinetics for grinded catalyst. Dotted lines are first order fits in term of liquid reagent concentrations.

It may seem peculiar that only two kinetic experiments are presented. Proper kinetic experiments typically require a variation of feed concentration, pressure, degree of grinding, stirring speed, etc. Some of these were included, but in the view of the objectives of this study, they are not necessary and even undesirable, since it will be attempted to measure wetting efficiency without an excessive kinetic decription. Batch experiments were only performed to find a region where Table 5.1 is applicable. External and even internal mass transfer limitations may have influenced rate measurements of the linear octene hydrogenation and the reaction may be faster than estimated, but this is not important in view of the requirements listed in Table 5.1. What is more important is the rate isooctene hydrogenation. It can be said that external mass transfer resistances did not influence the rate of this reaction, since a rate constant of more than 20 times higher was measured in the same experiment. Also, even for this reaction, the requirements for ϕ_{G2} allow for some error in the estimation of k_{r2}. The constraint of $1.5 \leq \phi_{G2} \leq 3.6$ translates to $0.1 \leq k_{r2} \leq 0.5\text{s}^{-1}$. It can be said with reasonable certainty that this is indeed the case.

5.3 Pilot studies

5.3.1 Experimental

Trickle-bed reactor setup

A schematic of the experimental setup is shown in Figure 5.3. The setup is designed to provide for gas-liquid upflow, gas-liquid downflow and countercurrent flow. The liquid reaction mixture, containing $\sim 1\%$ linear octene isomers and $\sim 2\%$ isooctene isomers, is pumped with a Bran & Luebbe H2-31 diaphragm metering pump capable of delivering $70\,\ell/\text{min}$ at 80 bar. The liquid feed is preheated to the reaction temperature before entering a 50 mm I.D., 1000 mm length reactor. The reactor walls are temperature controlled using three external heaters with wall thermocouples. Eight internal thermocouples are used as illustrated in Figure 5.4 to measure internal temperatures and verify isothermal operation. A Rosemount model 3051CD differential pressure transmitter is used for pressure-drop measurements to check for flow stability. A distributor with a drip point density of $11000\,\text{m}^{-2}$ is situated at the top of the reactor to ensure good liquid and gas distribution for trickle flow runs. If the liquid and gas enter through the bottom of the reactor (during upflow runs), these are distributed only by a retaining sieve plate and the packing itself.

Nitrogen and hydrogen can be fed to the reactor, the flow rates being controlled by 0-30 ℓ/min Brookes mass flow controllers. The maximum operating pressure of the system is 80 bar. A water-cooled heat exchanger is installed in the product line to cool down the product to approximately 30°C. Pressure is regulated with a back pressure regulator and monitored with pressure indicators and transducers at strategic points in the system. Samples are taken in a sampling bomb with a diptube for gas-liquid separation. Based on the high boiling points of the liquid components, it can be assumed that evaporation and the entrainment of liquid product in the gas will not significantly affect the product composition at 30°C. The product stream can either be recycled to the feed tank or routed to the product tank.

Experimental conditions and procedure

For each experimental run, the olefins in the liquid feed were hydrogenated over a packed bed with the catalyst described in section 5.2, diluted with inert $\gamma-Al_2O_3$ supports[3] of the same shape. All experiments were performed for five different liquid flow rates, corresponding to superficial velocities of 1.8, 2.6, 3.6, 4.5 and 7.5 mm/s; and three different flow configurations, namely upflow, Levec pre-wetted trickle flow and extensively pre-wetted trickle flow. The start-up procedure for each type of flow configuration is as follows:

[3]From batch experiments, it was found that the supports catalyse double-bond isomerisation. Since all double-bond isomers can be viewed as one reagent, the supports can be still be regarded as inert.

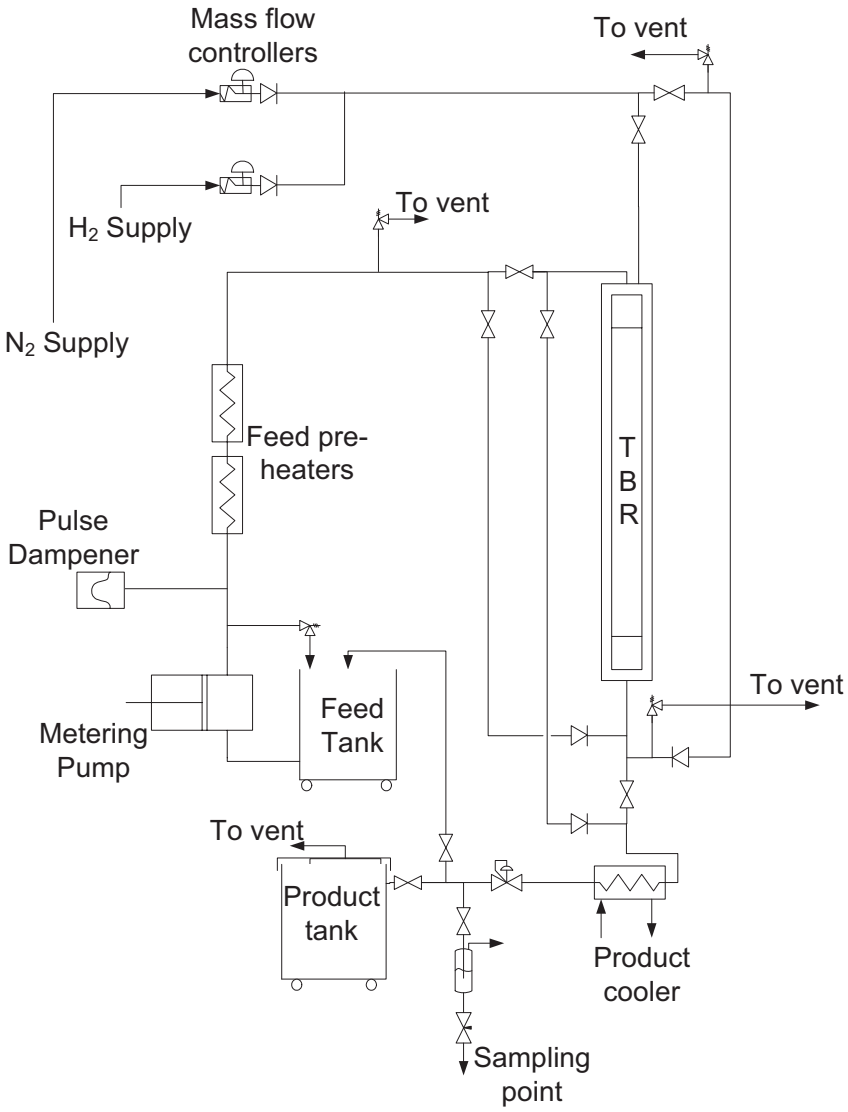

Figure 5.3: Schematic of the trickle-bed facility.

- *Upflow.* The liquid flow is set to the required rate by adjusting the pump stroke length and pump motor speed, and is fed to the bottom of the reactor, exiting at the top. Temperature control setpoints for the liquid feed preheaters and reactor heaters are set to the required temperatures. Nitrogen gas flow is introduced and the liquid is recycled to the feed tank until flow and temperature steady state are reached. Once steady state has been achieved, the product stream is rerouted to the product tank, nitrogen flow is shut off and hydrogen is introduced to the reactor. The feed tank is stirred, to ensure that the composition of the feed entering the reactor stays constant.

- *Levec pre-wetted trickle flow.* After the bed is flooded by feeding liquid in upflow,

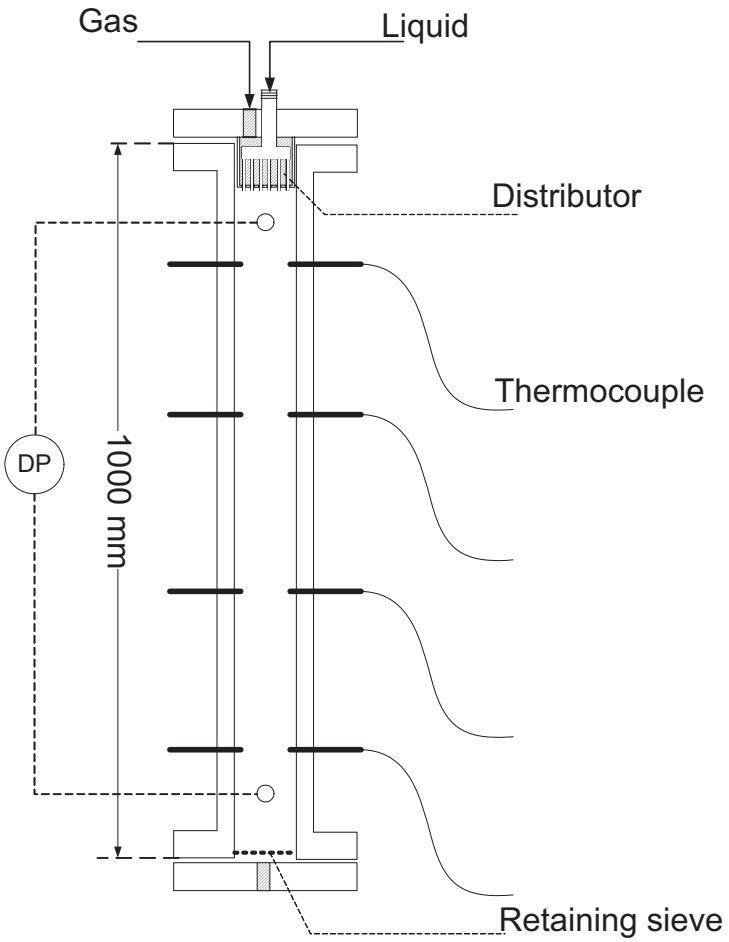

Figure 5.4: Reactor detail.

the liquid in the reactor is purged with nitrogen at atmospheric pressure, until no liquid can be detected in the reactor exit stream. The reactor is then pressurised with nitrogen to the required pressure, after which liquid is introduced to the top of the reactor at the required flow rate. It is ensured that the reactor pressure stays constant during the introduction of the liquid. The rest of the start-up procedure is the same as for upflow.

- *Extensively pre-wetted trickle flow.* The reactor is flooded by feeding liquid at the required rate to the bottom of the reactor under recycle conditions, until no gas can be detected in the reactor exit stream. The liquid feed configuration is then changed from upflow to downflow, and nitrogen is introduced to the reactor. The rest of the start-up procedure is the same as for upflow. This pre-wetting procedure will in most cases result in operating on the upper boundary of the multiplicity envelope (Loudon et al., 2006). Note that the pre-wetting procedure here differs from the procedure for extensive pre-wetting in Chapter 3. According to van der Merwe (2008), both pre-wetting procedures have the same hydrodynamic behaviour.

The above start-up procedures require a measure for steady state before nitrogen can be replaced by hydrogen. Steady state was verified by thermocouple readings, pressure drop and flow rate measurements: Once temperature and pressure-drop steady state is reached, the liquid flow rate in the product stream is repeatedly measured with a graduated cylinder and a stopwatch. If the product liquid flow rate stays constant, it is assumed that liquid holdup in the reactor stays constant and therefore that hydrodynamic stability has been reached. This takes between 10 and 20 system residence times, depending on the flow rate and configuration.

While switching over from nitrogen to hydrogen, the flow in the reactor can be disturbed. It is therefore important to choose the nitrogen and hydrogen flow rates in such a way that the disturbance is minimised. It was found that starting up with a volumetric nitrogen flow rate of roughly 60% that of the required hydrogen flow rate led to the smallest disturbances in terms of pressure drop and temperature. This is somewhat higher than is suggested by Ergun's equation for a minimum in pressure drop disturbance (25%-50% at the employed flow rates), since disturbance in bed temperature should also be kept as low as possible. For each experiment, at least 50% stoichiometric excess of hydrogen is fed to the reactor. With the highest conversions reported in this paper, this translates to at least 4.5 times the amount that has reacted. Experimental liquid and gas linear velocities through the reactor are shown in Figure 5.5. It is clear from the figure that all downflow experiments were performed in the trickle flow regime where incomplete wetting occurs. All experiments were performed at 60°C and 50 bar.

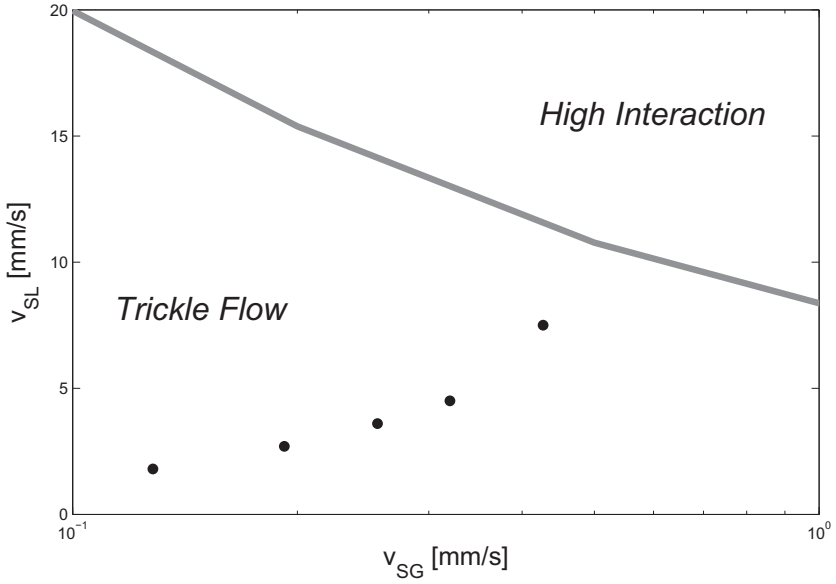

Figure 5.5: Flow map of experimental flow conditions. Adapted from Larachi et al. (1999). Hydrodynamic simulator available at http://www.gch.ulaval.ca/bgrandjean, accessed 22 May 2009

Two product samples were taken for each specific flow rate and configuration. The first sample was taken 10 reactor residence times (based on void volume) after achieving steady state under reaction conditions; and the second one 3-5 residence times later. The second sample serves to verify steady state conditions in the reactor.

Samples were analysed with an Agilent Technologies 6890 gas chromatograph (GC) fitted with a flame ionisation detector (FID). Elutriation was established on a 50 m-long Pona column with a 0.2 mm inner diameter and a 0.5 mm film thickness, using N_2 as carrier gas at a flow rate of 25 $^{ml}/_{min}$. A split ratio of 100:1 was used. The initial column temperature was 40°C, where it was held for 5 minutes. Then the temperature was ramped for 15 minutes at 4°C/min to obtain a good separation of the C_8 reagents, after which the temperature was increased to 300°C at 25°C/min.

Both the catalyst and support were supplied by Hereaus. A 630 mm bed of 70 g catalyst diluted with inert γ-Al_2O_3 supports was packed between two layers of 140 mm of inert supports at the entrance of and exit to the reactor. For a conversion of $X \leq 0.6$, the dispersion criterion of Sie and Krishna (1998) suggest a minimum reactor length of 550 mm for dispersion to be negligible in all modes of operation if the reaction is first-order. Bed porosity was 0.4 for all experiments.

Gas mass transfer resistances

To be able to adopt first-order kinetics by neglecting any influences that hydrogen may have on the reaction rate, it should first of all be ensured that the liquid entering the bed is saturated with hydrogen, independent of the liquid flow rate and flow configuration. For all experiments, 140 mm of inert supports were used to provide for hydrogen saturation before entering the bed. That this amount of support was indeed enough to ensure saturation was verified experimentally: two experimental runs were performed, one with an undiluted (70 g) catalyst bed situated 140 mm from the top reactor inlet and another with the bed situated close to the bottom of the reactor (the depth of the bed was 715 mm - 775 mm). The available area for gas-liquid mass transfer before entering the catalyst bed was far more in the former than in the latter case for gas-liquid upflow, and vice versa for trickle flow. The results for linear octene hydrogenations in these beds are shown in Figure 5.6. Since these two runs agree satisfactorily for all experimental conditions, it can be assumed that the liquid is saturated with the gas before entering the bed. Both experiments were repeated with good repeatability.

To ensure that any resistances to gas mass transfer within the catalyst bed are negligible, the hydrogenation of a 1% linear octenes and 2% isooctenes feed was compared with the hydrogenation of 0.5% linear octenes and 0.5% isooctenes. If gas mass transfer resistances play a role, the conversions for the lower concentration feed will be the highest. The results are shown in Figure 5.7. Close agreement between the results confirms that

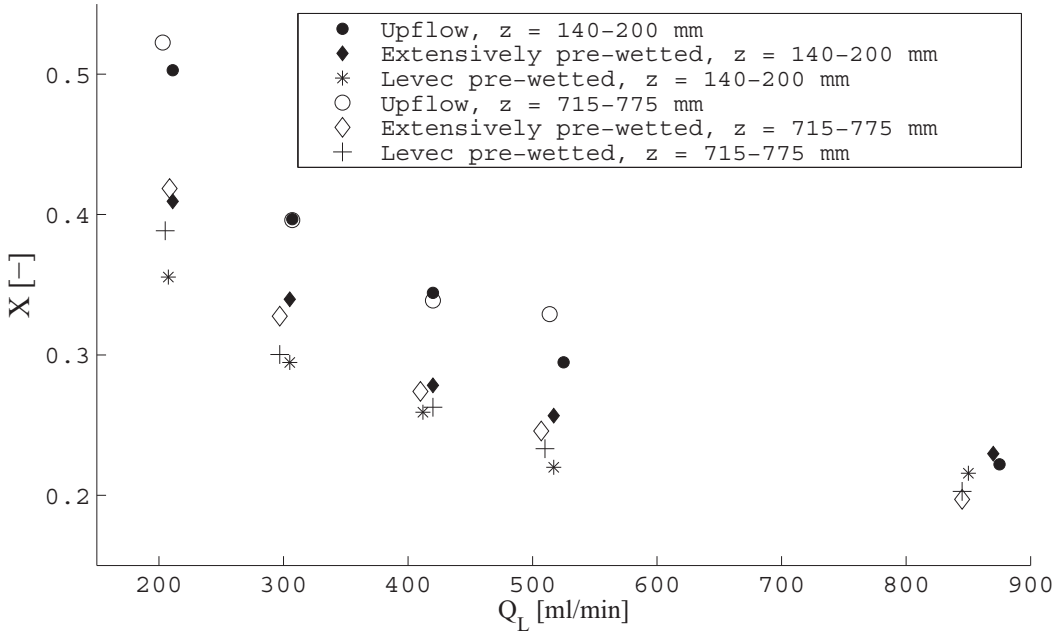

Figure 5.6: Test for saturation of liquid with hydrogen before entering the catalyst bed. The quantity z refers to the position of the bed as measured from the top.

hydrogen mass transfer can be ignored. The results also confirm the first-order behaviour of the reactions in terms of the liquid reagents.

5.3.2 Results and discussion

Conversion data

Typical conversion data for an experimental run are shown in Figure 5.8. In the rest of the discussion, an "experimental run" refers to two conversion datapoints for both reactions at five different liquid flow rates for all three different modes of operation. All the datapoints from an experimental run were generated consecutively (in no specific order) without interruption. Conversion data for the two different reactions are of course generated in parallel. In total, nine experimental runs were performed, each consisting of a total of 60 conversion measurements (30 product samples containing linear and isooctenes for 15 different flow conditions).

At all the liquid flow rates and for both reactions, conversion decreases in the order upflow- extensively pre-wetted trickle flow - Levec pre-wetted trickle flow at the same liquid flow rate. Although both reactions are known to be first-order in terms of the olefin concentration, none of the data shows good first-order behaviour for the fastest reaction, and conversion rates increase with liquid flow rate. For the slower reaction, the upflow conversion data approximates first order behaviour.

These observations are clear indicators that external liquid-solid mass transfer affects

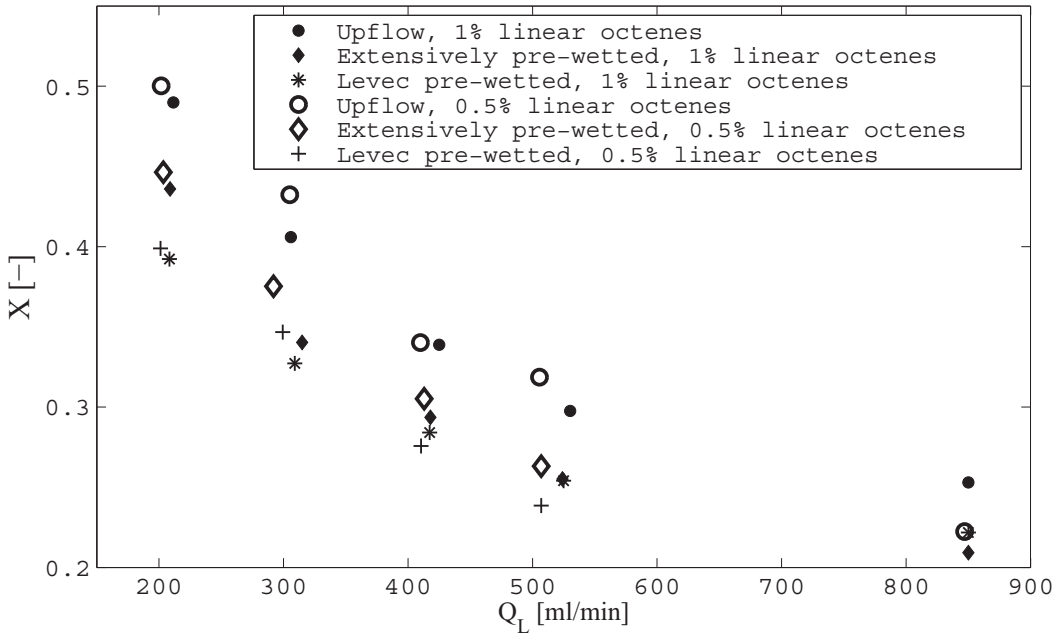

Figure 5.7: Conversion of linear octenes for feed concentrations of 0.5% and 1% linear octenes. The feed also contained 0.5% and 2% isooctenes, respectively

the reaction system: rates are slower at lower liquid velocities, and reaction inhibition is more pronounced for the fast reaction than for the slow reaction. Where upflow conversion data for the slow reaction approximate first-order behaviour, significant deviations still persist in trickle flow at low liquid flow rates. This can be due to even slower mass transfer rates in this mode of operation or incomplete wetting, or a combination of both. Since both reaction are known to be first order in terms of the non-volatile reagents, it is assumed that all deviations from first order behaviour can be ascribed to hydrodynamic effects, and the reactor design equation for both reactions can be written as:

$$\begin{aligned} -\ln(1-X) &= \frac{k_T.V_{cat}}{Q_L} \\ \text{Where} \quad V_{cat} &= m_{cat}/\rho_{cat} \end{aligned} \tag{5.3}$$

where k_T is a function of the hydrodynamic properties of the system and can be affected by the rate of liquid-solid mass transfer, or the wetting efficiency, or both. Since both external mass transfer and particle efficiency are linearly affected by the wetting efficiency,

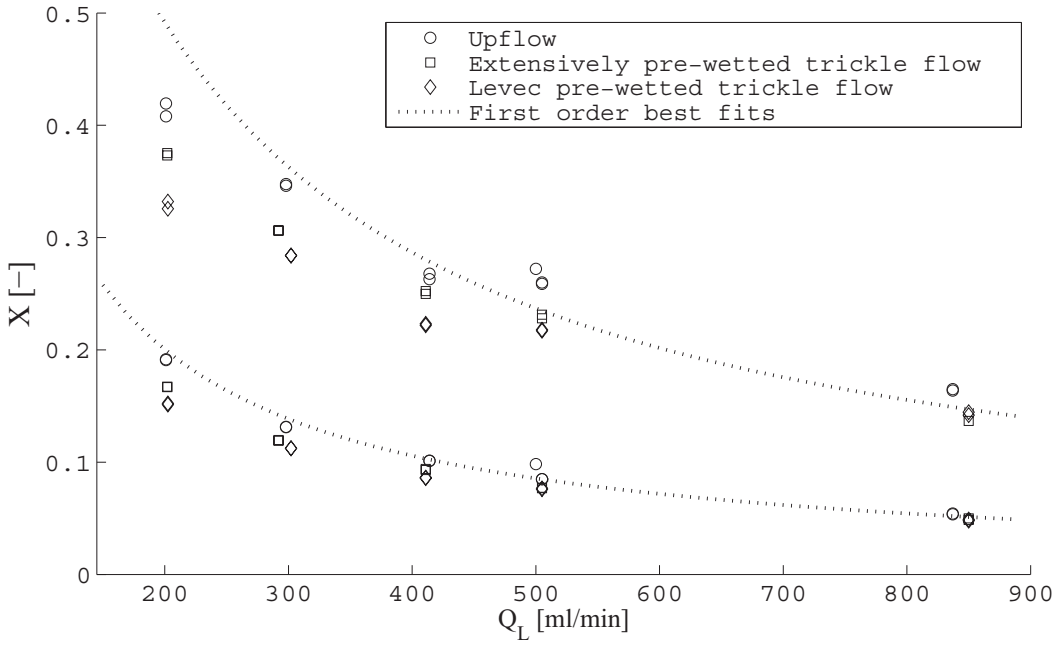

Figure 5.8: Typical conversion versus flow rate dataset for an experimental run.

k_T can be written as:

$$\begin{aligned} k_T &= \frac{(f.k_R).k_{LS}(a.f)}{(f.k_R)+k_{LS}(a.f)} \\ &= f\frac{k_R k_{LS} a}{k_R + k_{LS} a} \\ \text{Where} \quad a &= 6/d_p \\ k_R &= k_r \frac{V_R}{V_p}\,\eta|_{f=1} \end{aligned} \tag{5.4}$$

Equation (5.4) will be used in the treatment of conversion data. Note that for the rest of the discussion, k_T is specific to each conversion datapoint.

Although the characteristics of Figure 5.8 were highly repeatable for most of the experimental runs, only a few experimental runs were quantitatively repeatable. An example of how the conversion data varied from one experimental run to another is shown in Figure 5.9. The large scatter is attributed to differences in catalyst activity. Two types of activity variations are possible: one where the catalyst activity varied within a run, and another where the catalyst was stable during a run, but at a different activity than during other experimental runs. Data from the former type of activity variation can not be used, whereas data from the latter type can still be useful if treated correctly. For the selection of useful conversion data, it is first of all necessary to discard all data from experimental runs during which the catalyst deactivated. Deactivation of the catalyst while performing an experimental run might influence the interpretation

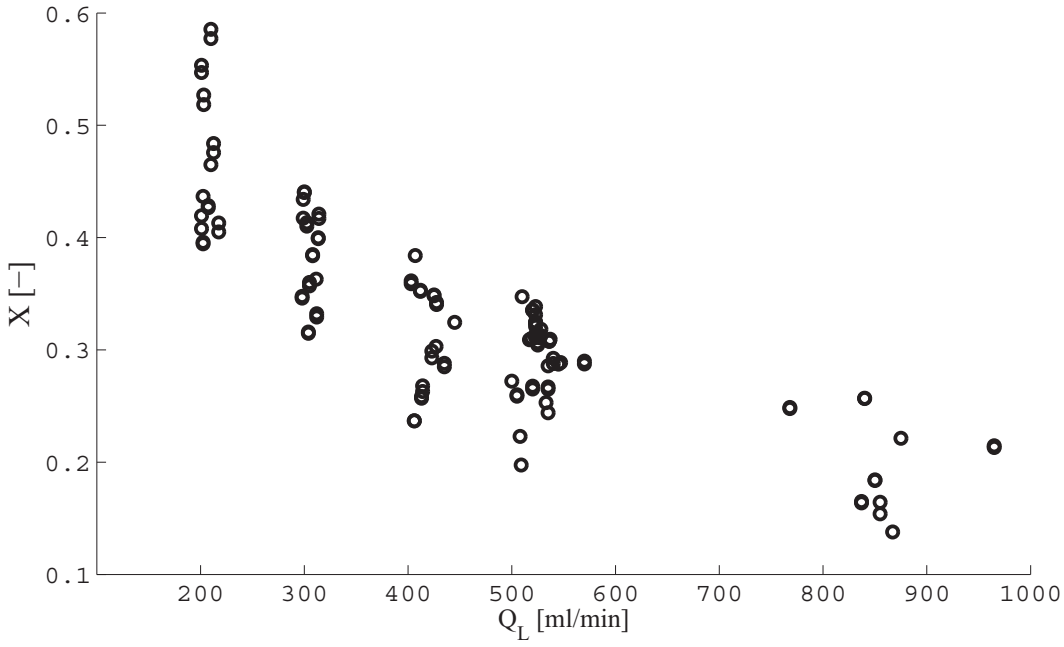

Figure 5.9: Unrefined upflow conversion data for the hydrogenation of linear octenes.

of hydrodynamics. For an indication of catalyst stability during an experimental run, the following catalyst activity indicator (CAI) was defined, which can be calculated from conversion data without any knowledge of the reaction rate constants (using the equation on the right):

$$\text{CAI} = \frac{k_{R1}.k_{R2}}{k_{R1} - k_{R2}} = \left.\frac{k_{T1}k_{T2}}{k_{T1} - k_{T2}}\right|_{\text{upflow}} \tag{5.5}$$

The derivation of above Equation is shown in Section 5.3.3 (Equations 5.7 and 5.8), where it is used for the estimation of wetting efficiency. For complete wetting in the upflow mode, the CAI should be independent of liquid flow rate under liquid-limited conditions, and is directly related to the catalyst activity. All experimental runs during which the CAI decreased notably, were discarded. An example of how the CAI is used is shown in Figure 5.10.

Because of catalyst deactivation, data from four of the nine experimental runs had to be discarded. Most of the discarded datasets were from experiments where a new catalyst bed was packed. Although all of the retained datasets were generated with stable catalyst, the stable catalyst activity varied from one experimental run to another, as seen in Figure 5.11. It is therefore important to develop methods for the estimation of liquid-solid contacting which are insensitive to the specific catalyst activity.

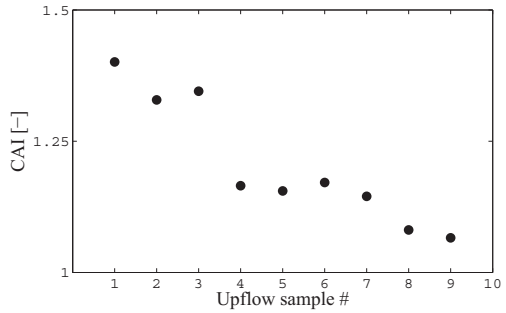

(a) An example of an experimental run for which the CAI indicates a drop in catalyst activity. All data generated during this run were discarded.

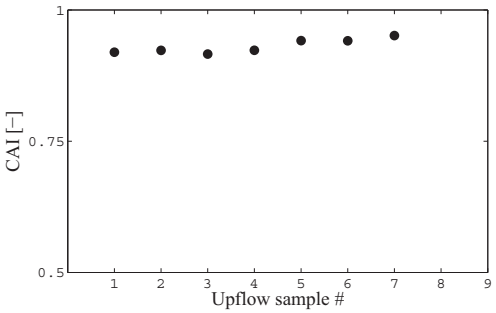

(b) An example of an experimental run with stable catalyst. The dataset generated during this experimental run can be used.

Figure 5.10: Catalyst stability checks

5.3.3 Wetting efficiency

Consider two first-order reactions with effective kinetic rate constants k_{R1} and k_{R2} occurring in a trickle bed reactor as modelled in Equation (5.4). From the effective rate constants k_{T1} and k_{T2} obtained from conversion data, the liquid mass transfer coefficient can be calculated twice for known reaction rate constants and wetting efficiency:

$$k_{LS}a = \frac{k_{T1}k_{R1}}{f.k_{R1} - k_{T1}} = \frac{k_{T2}k_{R2}}{f.k_{R2} - k_{T2}} \tag{5.6}$$

Note that Equation (5.6) is only valid if both reactions take place under the same hydrodynamic conditions, and refers to the treatment of one specific conversion datapoint in terms of liquid flow rate and catalyst activity. The relationship also relies on the assumption that the molecular diffusivity of both reagents is the same, which was established as holding true.

By rearranging Equation (5.6), it is possible to calculate wetting efficiency at a specific hydrodynamic state (mode of operation and liquid flow rate) if k_{R1} and k_{R2} are known.

$$f = \underbrace{\frac{k_{R1} - k_{R2}}{k_{R1}k_{R2}}}_{A} \cdot \underbrace{\frac{k_{T1}k_{T2}}{k_{T1} - k_{T2}}}_{B} \tag{5.7}$$

For constant catalyst activity, part (B) of Equation (5.7) is directly proportional to wetting efficiency and should be constant during upflow operation if the assumption of complete wetting in upflow operation holds true, so that:

$$\frac{k_{R1} - k_{R2}}{k_{R1}k_{R2}} = \left.\frac{k_{T1} - k_{T2}}{k_{T1}k_{T2}}\right|_{upflow} \tag{5.8}$$

Compare Equation (5.8) to the definition of the CAI in Equation (5.5). Since the CAI did

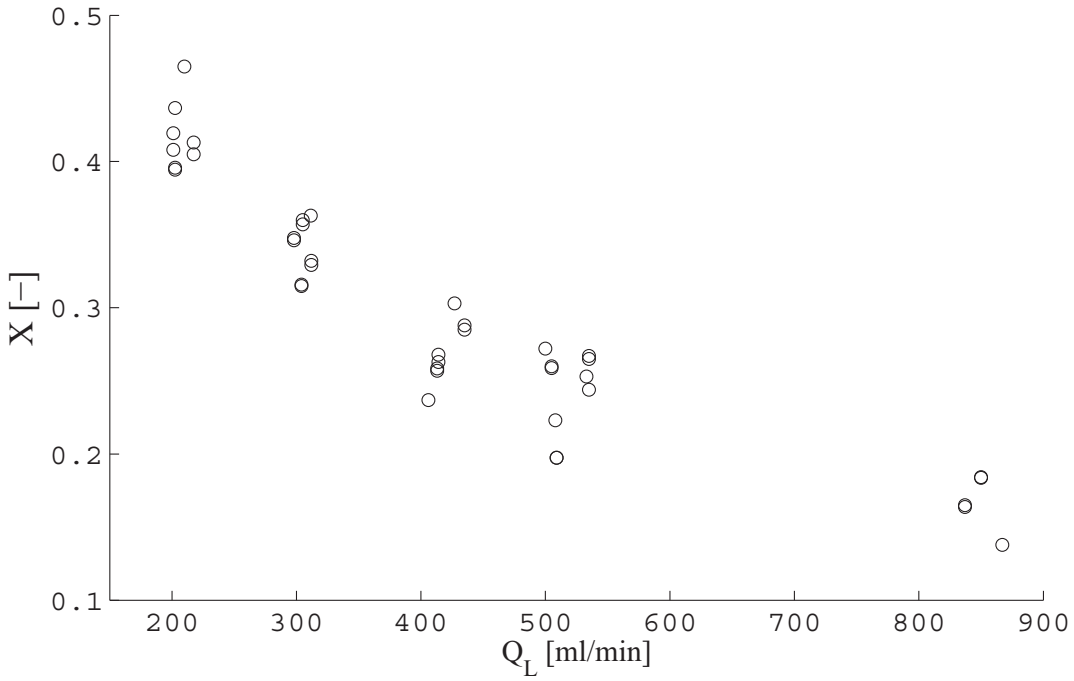

Figure 5.11: Upflow linear octene conversion data from experimental runs with stable catalyst

not show any correlation with liquid flow rate and was constant as long as the catalyst activity remained constant, complete wetting in upflow operation can be assumed. Wetting efficiencies in trickle-flow operation can therefore be calculated if conversion data is available for upflow operation at the same catalyst activity.

$$f_{TBR} = \left.\frac{k_{T1}k_{T2}}{k_{T1}-k_{T2}}\right|_{TBR} \left.\frac{k_{T1}-k_{T2}}{k_{T1}k_{T2}}\right|_{upflow} \tag{5.9}$$

Note that for the calculation of wetting efficiency, no knowledge of the kinetic rate constants k_{R1} and k_{R2} is required, and it is possible to calculate wetting efficiency from the raw conversion data as long as upflow conversion data is available at the same catalyst activity, i.e. the catalyst was stable during an experimental run. Note that it is not necessary to have upflow data available at all liquid flow rates: only one upflow conversion datapoint for both reactions is needed to calculate the quatinity defined in equation (5.8), as long as the catalyst was stable during an experimental run.

All measured wetting efficiencies as calculated with Equation (5.9) are shown in Figure 5.12. For easy comparison of Levec- and extensively pre-wetted trickle flow, averaged wetting efficiencies are shown in Figure 5.13. As expected from Chapter 3, hydrodynamic multiplicity is the most severe (about 10-15% variation) at low liquid velocities, where liquid flow in Levec pre-wetted beds tends to channel. The wetting efficiency correlation suggested by Julcour-Lebique et al. (2009) is shown by a dotted line. This correlation was developed from an extensive set of wetting efficiency data which were exclusively

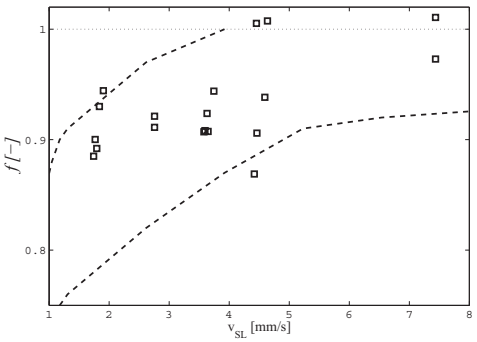

(a) Wetting efficiency measurements for extensively pre-wetted trickle flow.

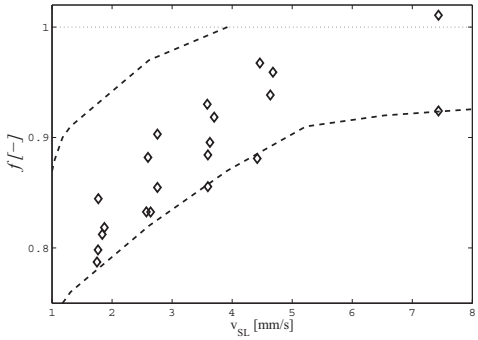

(b) Wetting efficiency measurements for Levec pre-wetted trickle flow.

Figure 5.12: Measured wetting efficiencies as a function of liquid superficial velocity. Dotted lines indicate the estimations of wetting efficiencies by Satterfield (1975)

measured by a colorimetric method. It is reassuring that the results from this technique compare so well with the pilot reactor measurements[4]. Quantitatively, the results from Chapter 3 differ significantly from the current results. The most obvious difference between the two systems that were used is the difference in surface tension of the liquid (2.5 times more for water than for the current reaction mixture). Surface tension was suggested to be the reason for differences in reactive wetting efficiency measurements by Leung et al. (1987) and Morita and Smith (1978). Still, the correlation shown here cannot explain the differences in measured wetting efficiencies, though some colorimetric data by the same authors do coincide with the measurements in Chapter 3 (Baussaron et al., 2007).

5.3.4 Liquid-solid mass transfer

Based on the fact that differences in catalyst activity affected conversion rates of the linear octenes, it can be concluded that even this (fast) reaction is not completely limited by the rate external liquid-solid mass transfer. Contrary to the estimation of wetting efficiency, approximations of effective kinetic rate constants k_{R1} and k_{R2} are therefore needed to estimate mass transfer rates from conversion data. However, liquid-solid mass transfer coefficients should be independent of the reaction rates and be a function of liquid flow rate only, provided that all liquid and bed properties are constant and the effect of gas flow is negligible. For all experiments, the gas flow rate was very low, as can be seen in Figure 5.5. Most liquid-soled mass transfer correlations have the following functional relationship with the liquid flow rate:

$$k_{LS}a = k_0 Q^{k_1} \tag{5.10}$$

[4]Liquid-solid mass transfer measurements, for example, seem to be sensitive to the measurement method.

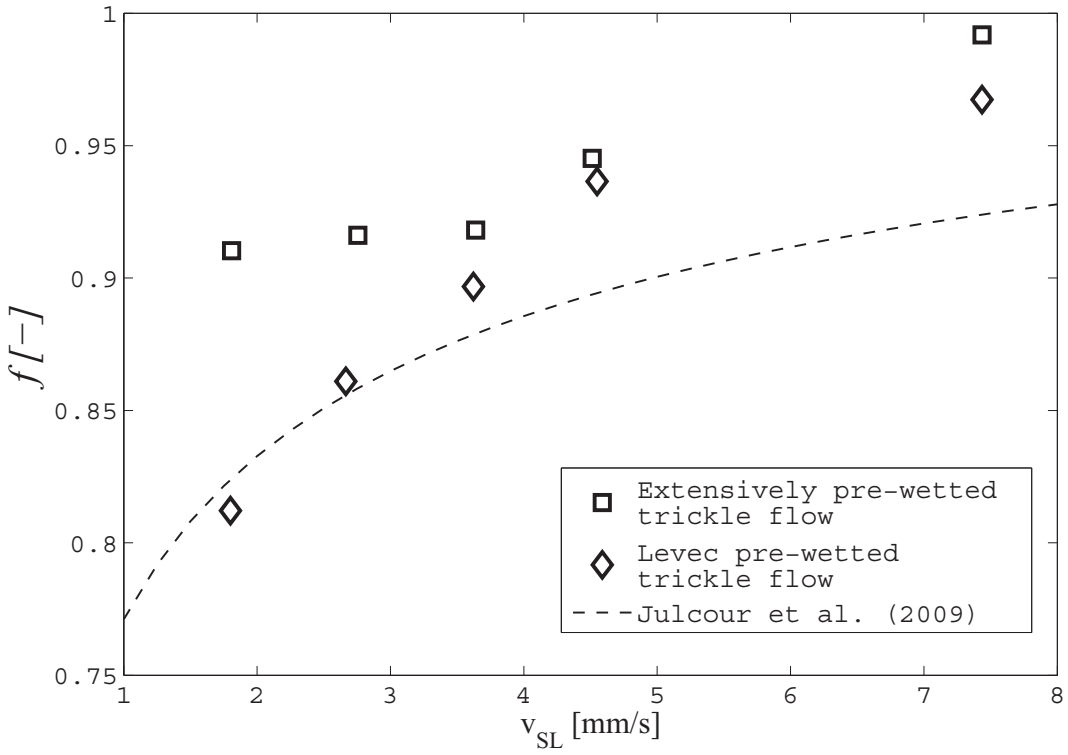

Figure 5.13: Averaged wetting efficiency for trickle flow operation as a function of liquid superficial velocity.

Based on this relationship, the apparent rate constant at a specific liquid flow rate in upflow operation will, according to Equation (5.4), be equal to:

$$k_{Tx,ij} = \frac{k_{Rx,i} k_0 Q_j^{k_1}}{k_{Rx,i} + k_0 Q_j^{k_1}} \tag{5.11}$$

Where x = 1 for linear octene hydrogenation
x = 2 for isooctene hydrogenation
i refers to a specific experimental run
j refers to the liquid flow rate

The coefficiencts k_0 and k_1 should be independent of the reaction rates, and the following function was minimised in order to obtain approximations of *(a)* kinetic rate constants for both reactions x and all experimental datasets i, and *(b)* liquid-solid mass transfer for upflow operation as a function of liquid flow rate:

$$F = \sum_{xij} \left| X_{xij} + \exp\left(\frac{k_{Rx,i} k_0 Q_j^{k_1 - 1} . V_{cat}}{k_{Rx,i} + k_0 Q_j^{k_1}} \right) - 1 \right| \tag{5.12}$$

The minimisation of this function is an iterative procedure, where $k_{R,xi}$ is fitted onto conversion dataset i specific to reaction x with set values for k_0 and k_1 (1 parameter fitted to 10 datapoints), and k_0 and k_1 are fitted to all conversion datasets with $k_{R,xi}$ set for each dataset/reaction (2 parameters fitted to 100 datapoints). Figure 5.14 shows the datafits obtained with this procedure. The estimated values for k_{R1} and k_{R2} (based on catalyst volume), vary between 0.11 and 0.05, and 0.015 and 0.01 s^{-1} respectively. These correspond to $1.2 \leq \eta \cdot k_{r1} \leq 0.55$ and $0.11 \leq \eta \cdot k_{r1} \leq 0.17$. For the isooctene hydrogenation, these values agree well with the batch experiments, since $\eta \approx 1/\phi_G$. The estimated higher limit of linear octene hydrogenation is much higher than the batch experiments suggest (the results from batch experiments correspond to the lower limit). Accurate estimations of very high kinetic rates for the determination of liquid-solid mass transfer are not too important, since the reaction will become more and more limited by external mass transfer rates.

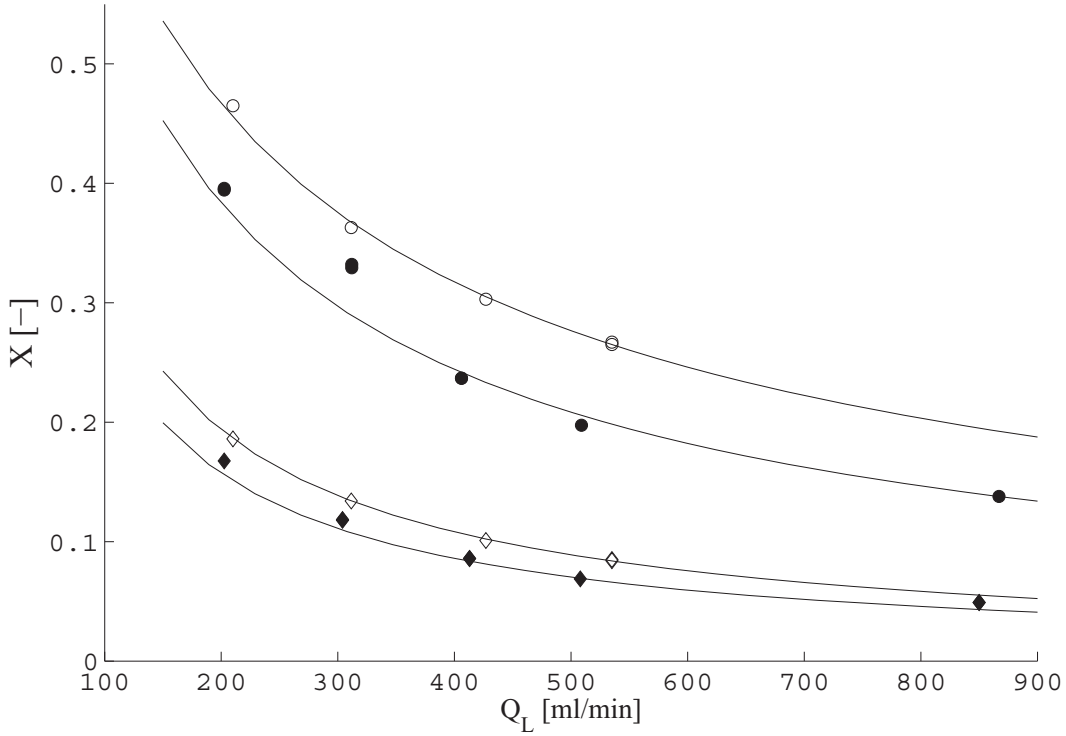

Figure 5.14: Fits of upflow conversion data obtained from minimising equation (5.12). The highest and lowest catalyst activity cases are shown.

Now that estimations of the effective kinetic rate constants are available, mass transfer coefficients can be calculated for all flow rates and operating modes by substituting Equation (5.7) into Equation (5.6):

$$k_{LS}a = \frac{k_{T1} - k_{T2}}{k_{T2}/k_{R2} - k_{T1}/k_{R1}} \tag{5.13}$$

With the wetting efficiency results from the previous section, it is also possible to calculate mass transfer coefficients directly with equation (5.6). Equation (5.13) is preferred, so that mass transfer rates can be calculated without making use of the wetting efficiency results. Liquid-solid mass transfer coefficients calculated with Equation (5.13) are independent of the wetting efficiency and an indication of the specific rate of mass transfer at any specific point in the bed. Most liquid-solid mass transfer studies in trickle-beds are based on either a dissolution (Sylvester and Pitayagulsarn, 1975; Dharwarkar and Sylvester, 1977; Specchia et al., 1978; Lakota and Levec, 1990) or an electrochemical method (Hirose et al., 1976; Chou et al., 1979; Sims et al., 1993; Latifi et al., 1997; Trivizadakis and Karabelas, 2006). These experimental methods lead to mass transfer coefficient measurements which include wetting efficiencies, i.e. usually $k_{LS} \times f$ is measured. To calculate $k_{LS} \times f$, one can once again use Equations (5.6) and (5.7) to find the following relationship:

$$k_{LS}a.f = \frac{k_{R1} - k_{R2}}{k_{R1}/k_{T1} - k_{R2}/k_{T2}} \tag{5.14}$$

For upflow where $f = 1$, Equation (5.13) and (5.14) should yield the same results, which can be used as a test whether the estimated reaction rate constants and the assumption that $f = 1$ in upflow operation are reasonable. That this is indeed the case is shown in Figure 5.15, which is a parity plot of upflow mass transfer rates calculated via equation (5.13) and via equation (5.14). Average wetting efficiency-based ($k_{LS}f$, Equation 5.14) and specific (k_{LS}, Equation 5.13) liquid-solid mass transfer coefficients for trickle-bed operation are shown in Figure 5.16. Overall, hydrodynamic multiplicity gave rise to about 10 - 20% variation in $k_{LS}f$. The correlations of Dharwarkar and Sylvester (1977) and Latifi et al. (1997) are also shown. The former was developed from a large database, while the latter is recommended by Dudukovic et al. (2002) for trickle-bed design purposes and was developed from electrochemical-based data. However, many correlations, especially those developed from dissolution data, predict liquid-solid mass transfer coefficients as much as ten times smaller than reported in the figure.

The multiplicity behaviour of liquid-solid mass transfer in trickle beds has previously been explained as a combined liquid holdup - wetting efficiency effect **?**: At a specific superficial liquid velocity, a low liquid holdup should enhance mass transfer due to higher interstitial liquid velocities. On the other hand, low wetting efficiencies should be detrimental for mass transfer. That liquid holdup (interstitial velocity) and wetting efficiency (area for mass transfer) are not the only hydrodynamic properties that influence mass transfer rates, is clear from the inset in Figure 5.16. Though the specific mass transfer coefficients in this subfigure are not affected by wetting efficiency, a marked difference between Levec and extensively pre-wetted beds still persists. The differences cannot be explained in terms of interstitial velocity, since the liquid holdup in a Levec pre-wetted bed is generally lower than in an extensively pre-wetted bed, resulting in higher inter-

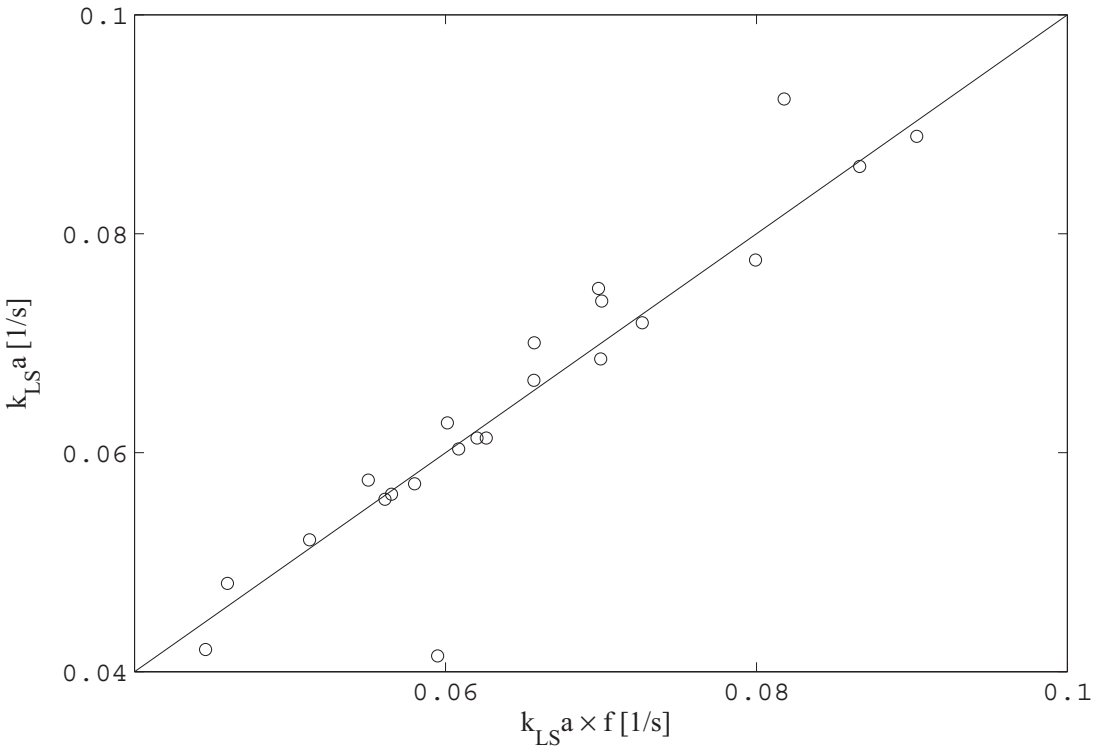

Figure 5.15: Parity plot for $k_{LS}a.f$ and $k_{LS}a$ for upflow operation. Good agreement confirms reasonability of estimated values for k_{R1} and k_{R2}, and that $f_{upflow} = 1$.

stitial liquid velocities. Still, the mass transfer coefficients are lower and the observed multiplicity behaviour of liquid-solid mass transfer is therefore related to the differences in flow structure. Several studies of trickle-flow hydrdynamic muliplicity have been reported where these differences were observed (Kan and Greenfield, 1979; Lutran et al., 1991; Ravindra et al., 1997a; van der Merwe et al., 2007). The findings are also in accordance to the findings in Chapter 3.

Lastly, liquid-solid mass transfer in trickle-flow operation is compared to mass transfer in upflow operation in Figure 5.17. Liquid-solid mass transfer coefficients for upflow operation are 12 to 30% higher than for trickle-flow operation at the same superficial liquid velocity, confirming that some flow characteristics in the trickle flow regime are detrimental to the overall liquid-solid mass transfer rates.

5.4 Conclusions

By using a simple first-order reaction model for two reactions occurring in parallel, wetting efficiency could be measured in a pilot trickle-bed reactor without the need for a proper kinetic description of the reactions. Measurements were based on conversion data for linear and isooctene hydrogenation. On the basis of theoretical considerations, some general criteria could be given for a reaction system to be suitable for wetting

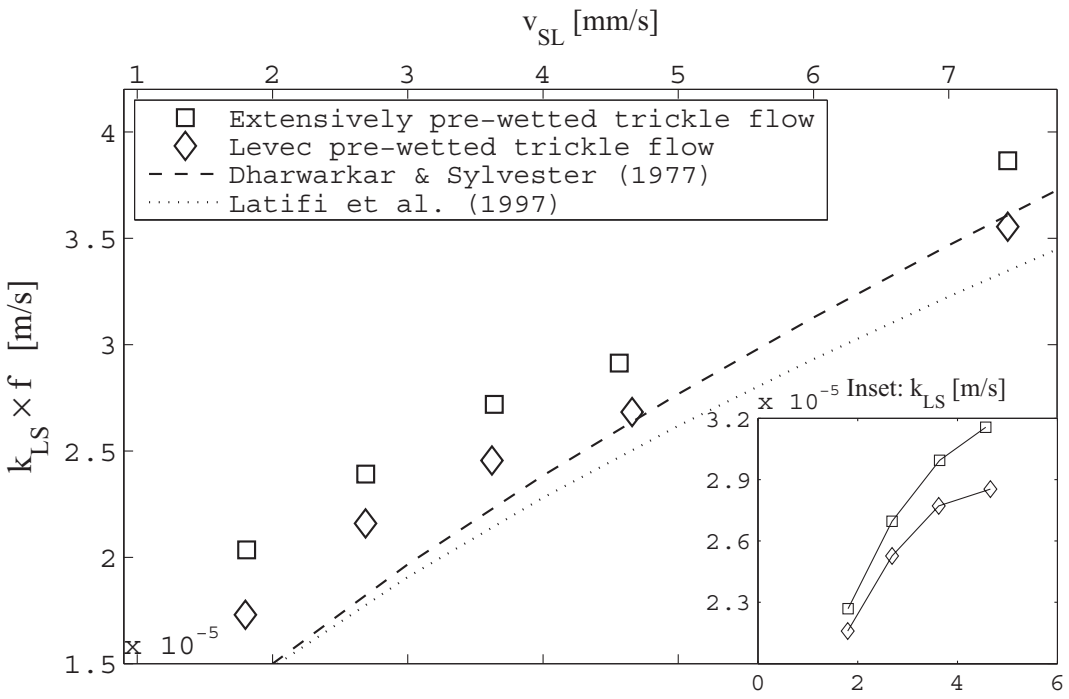

Figure 5.16: Averaged wetting efficiency-based liquid-solid mass transfer coefficients for trickle flow operation. Inset: Specific mass transfer coefficients.

efficiency measurements. With estimations of reaction rates, it was also possible to measure specific liquid-solid mass transfer coefficients, independently of the wetting efficiency measurements. The multiplicity behaviour of liquid-solid mass transfer coefficients suggests that different flow patterns exist that determine the characteristics of liquid-solid mass transfer in trickle flow, and that liquid-solid mass transfer cannot be simply related to interstitial liquid velocity. The multiplicity envelope shows up to 10% variation in wetting efficiency and 10% - 20% variation in mass transfer rates, both being higher for extensively pre-wetted beds. The results compare well with the colorimetric study in Chapter 3, the results of which also suggest different types of flow for Levec and extensively pre-wetted beds. Under liquid-limited conditions, upflow operation outperforms trickle flow operation at the same liquid flow rate, partly because of complete wetting, but also because of higher specific liquid-solid mass transfer coefficients.

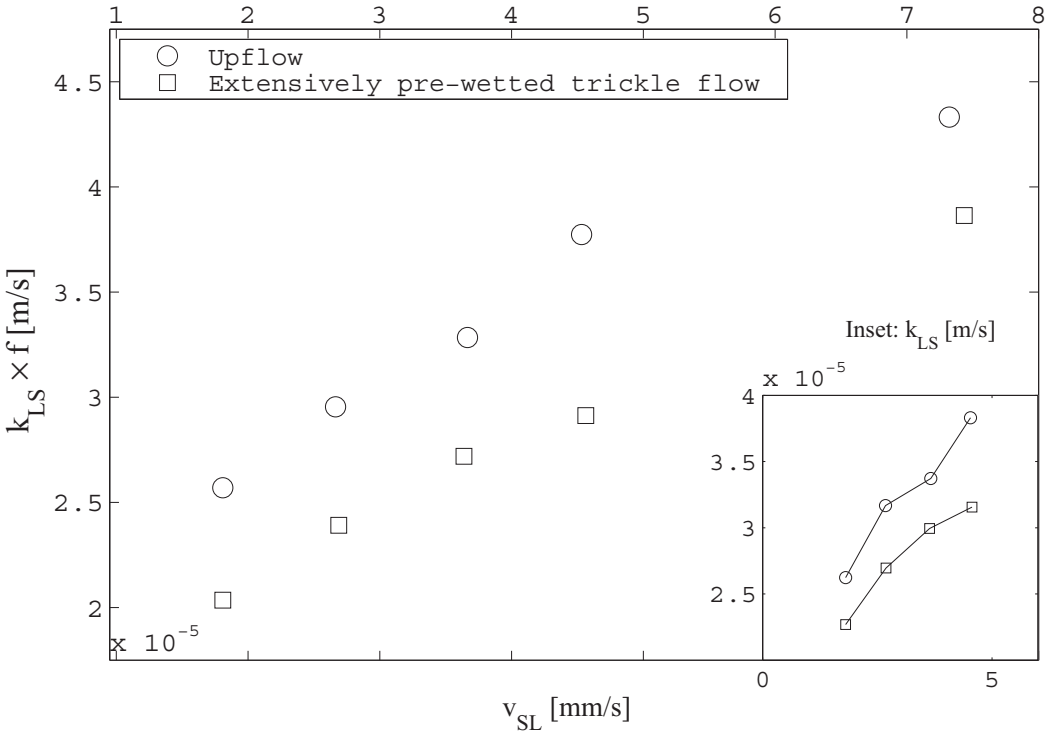

Figure 5.17: Comparison of liquid-solid mass transfer in trickle-flow and upflow operation. Inset: Specific mass transfer coefficents.

Nomenclature

a	area per volume of catalyst particle, $^1/_{\mathrm{m}}$
Bi	Biot number for a sphere, $Bi' = \frac{k_{LS} r_p}{D_{eff}}$
Bi'	modified Biot number, $Bi' = \frac{k_{LS} V_R}{S_P D_{eff}}$
D_{eff}	liquid reagent effective diffusivity, $^{\mathrm{m}^2}/_{\mathrm{s}}$
D	molecular diffusivity, $^{\mathrm{m}^2}/_{\mathrm{s}}$
d_p	catalyst pellet diameter, m
f	wetting efficiency, dimensionless
k_0	fitting constant for approximation of upflow external liquid-solid mass transfer
k_r	first-order reaction rate constant based on shell volume, s^{-1}
k_R	first-order reaction rate constant based on catalyst volume, s^{-1}
k_T	apparent first order reaction rate constant based on catalyst volume, s^{-1}
k_{LS}	liquid-solid mass transfer coefficient, $^{\mathrm{m}}/_{\mathrm{s}}$
m_{cat}	mass of catalyst particles in reactor, kg
Q_L	liquid volumetric flow rate, $^{\mathrm{m}^3}/_{\mathrm{s}}$ ($^{\mathrm{ml}}/_{\mathrm{min}}$ in figures)
S_P	pellet external area, m^2
V_{cat}	volume of catalyst in reactor, m^3
V_R	catalyst shell volume for an egghell catalyst, m^3
v_{Si}	superficial velocity of i-phase $v_{Si} = \frac{Q_i}{A_c}$, $^{\mathrm{m}}/_{\mathrm{s}}$
X	conversion, dimensionless
z	depth in reactor measured from top inlet, mm

Greek letters

ϕ_G	Generalised (Aris) modulus, $\phi_G = \frac{V_R}{S_p}\sqrt{\frac{k_r}{D_{eff}}}$
η	pellet efficiency factor, dimensionless
η_0	overall efficiency factor, dimensionless
ρ_{cat}	catalyst particle density, $^{\mathrm{kg}}/_{\mathrm{m}^3}$

Subscripts

1	refers to faster reaction
2	refers to slower reaction
i	refers to specific experimental run with stable catalyst
j	refers to specific flow rate
x	refers to specific reaction, either 1 or 2

CHAPTER 6

CLOSING REMARKS

Wetting efficiency and liquid-solid mass transfer effects in trickle-bed reactors were studied at three different levels. Fractional wetting in a TBR was characterized on a bed and particle scale in a non-reactive N_2-water experimental study, making use of colorimetry. The study illustrates multiplicity effects in terms of flow morphology and subsequently wetting efficiency, using particle-scale wetting distributions. These results correspond well with another study on wetting efficiency and liquid-solid mass transfer, performed in a high-pressure pilot trickle-bed reactor. Here, it was also found that pre-wetting had a major effect on partial wetting, while liquid-solid mass transfer results suggest different types of flow for the two boundaries of hydrodynamic multiplicity in pre-wetted trickle-bed reactors.

Liquid-solid contacting was also investigated at a particle-scale level. The wetting geometries obtained from the colorimetric study were used to investigate the effects of partial wetting on intraparticle diffusion, using FEM simulation. With FEM simulations, it is possible to study intraparticle diffusion and reaction using the fundamental description of this process. Using realistic geometries for partial wetting, realistic data could be generated regarding wetting efficiency and intraparticle diffusion. These data were used for simplified theoretical decriptions of liquid-solid contacting effects on a particle-scale level, which aided in the experimental planning of a reactive method for the measurement of wetting efficiency.

An important reason to study liquid-solid contacting from different angles, was to link hydrodynamic observations and theory to gain a sense of what to expect from a reactor under trickle-flow conditions. Though integrated to some degree and corresponding well with each other, the overall study leaves much scope for further investigation into how liquid flow morphology influences transfer processes in a trickle-bed reactor. For example, only the simple case of strong internal diffusion limitations under liquid-limited

conditions was considered in a reactor study, while many of the ideas from the study of intraparticle diffusion and reaction were left unexplored. A typical continuation of the reactor study would be to explore reactor behaviour over a large γ-range. For this reason, a preliminary study was performed under gas-limited conditions. Though some agreement was found with the work in the body of this report, unexpected behaviour was also found. For example, the liquid-solid mass transfer results from the liquid-limited study did not correspond to observed rates in the reactor or even with existing liquid-solid and gas-liquid mass transfer correlations. The study was not presented in the main body of this thesis, since it consists of limited data which would not suffice for a clear understanding of the reactor, but is reported in Appendix B. Though the work presented in this thesis elucidates liquid-solid contacting effects in gas-liquid packed bed reactors to some extent, this study is yet another indication that there is still room for improvement in the understanding of these reactors.

More specific contributions of this work include the following:

- Presentation of the distribution of particle wetting of a packed bed under different conditions in the multplicity envelope of trickle flow. This may help explain multiplicity behaviour of trickle-bed reactors.

- An easy-to-use model which can be used to model simultaneous rate-limiting behaviour of both volatile and non-volatile reagents in a trickle-bed reactor.

- A description for partial wetting effects on eggshell catalysts and the illustration that these differ from monodispersed catalysts.

- The development and implication of a wetting efficiency measurement method without the need of kinetic descriptions or estimations of external mass transfer.

- Estimation of wetting efficiency and liquid-solid mass transfer multiplicity behaviour under high-pressure reaction conditions relevant to industry.